Physics Letters A 377 (2013) 3223–3227

Contents lists available at ScienceDirect

Physics Letters A

www.elsevier.com/locate/pla

Langevin approach for stochastic Hodgkin–Huxley dynamics with discretization of channel open fraction

Yandong Huang [a], Sten Rüdiger [b], Jianwei Shuai [a,*]

[a] Department of Physics and Institute of Theoretical Physics and Astrophysics, Xiamen University, Xiamen 361005, China
[b] Institute of Physics, Humboldt-Universität zu Berlin, Germany

ARTICLE INFO

Article history:
Received 20 June 2013
Received in revised form 19 September 2013
Accepted 3 October 2013
Available online 9 October 2013
Communicated by C.R. Doering

ABSTRACT

The random opening and closing of ion channels establishes channel noise, which can be approximated and included into stochastic differential equations (Langevin approach). The Langevin approach is often incorporated to model stochastic ion channel dynamics for systems with a large number of channels. Here, we introduce a discretization procedure of a channel-based Langevin approach to simulate the stochastic channel dynamics with small and intermediate numbers of channels. We show that our Langevin approach with discrete channel open fractions can give a good approximation of the original Markov dynamics even for only 10 K^+ channels. We suggest that the better approximation by the discretized Langevin approach originates from the improved representation of events that trigger action potentials.

1. Introductions

Stochastic opening and closing of ion channels, known as channel noise, has become a central issue in computational neuroscience. Channel noise is thought to be functionally critical in different types of cells, such as in retinal ganglion cell [1], pancreatic β cells [2], hippocampal neurons [3,4], and cardiac myocytes [5,6]. In particular, at small membrane patch area the physiological effects of channel noise are quite noticeable.

In recent years, there has been much interest in the theoretical modeling of the probabilistic nature of ion-channel gating. Considering the small size of axonal membrane patches [7] and the stochastic channel dynamics, the Hodgkin–Huxley (HH) neuronal model can be accurately simulated with the Markov method [8–13]. However, the computational cost of a Markov-based model may be prohibitive, making approximate algorithms, such as a Langevin-like approach, advantageous.

Different Langevin approaches (LA) have been suggested so far according to how to incorporate the channel noise into the deterministic differential equations of the HH neuron model [14]. As an example, the K^+ channel has 4 identical n-gates to control the channel opening and closing dynamics. The total K^+ channel current is linearly related to the open channel fraction n^4, which can be calculated through discussing the dynamics of the single gate open fraction n or the transition dynamics of five channel state variables. By considering the Gaussian noise directly on the gate open fraction, Fox and Lu suggested a simple gate-based LA [15,16]. Due to its simplicity, such type of gate-based LA has been applied extensively to stochastic channel dynamics [17,10,11]. However, the past few years have seen increasing evidences pointing out apparent inaccuracies of gate-based LAs [18–24].

Alternatively, one may incorporate the Gaussian noise into the channel state fractions [16,25,26]. Fox and Lu proposed an approach by adding the channel noise on all the channel state variables [16], which will be termed as channel-based LA in the Letter. In this method, the master equations of the channel state fractions are perturbed by a Gaussian noise vector. A problem with this method is that the Gaussian noise may drive the channel state fractions out of the region of $[0, 1]$. Same problem occurs for the gate-based LA, but one can simply truncate the single gate variable into $[0, 1]$. While for channel-based LA, the challenge is how to keep the sum of the channel state fractions to be 1 after truncating channel state fraction into $[0, 1]$. The original channel-based LA ignores such problem, which is applicable for large channel number with less probability to go out of $[0, 1]$ in the simulation.

A reflection method was applied to the original channel-based LA to constrain the state fractions in the meaningful region of $[0, 1]$ [27]. However, this approach fails at K^+ channel number smaller than 500, because the method changes the mean values of the fractions of channel states produced by the original channel-based LA. Recently, another efficient channel-based LA was proposed to limit the state fractions in the region of $[0, 1]$ by truncating and then restoring the extra state fractions [28]. However, we still found that the method is inaccurate when the K^+ channel number is smaller than 50.

* Corresponding author. Tel.: +86 592 218 2575; fax: +86 592 218 9426.
E-mail address: jianweishuai@xmu.edu.cn (J. Shuai).

0375-9601/$ – see front matter
http://dx.doi.org/10.1016/j.physleta.2013.10.008

Originally, of course, the Langevin approach was developed for large channel numbers. An interesting but less often discussed question is if the Langevin method is still valid for small channel numbers. In this Letter, we suggest a Langevin approach, which is applicable at membrane patches with a small number of channels. At small channel number, the discretization effect of open fractions of the system could not be ignored. In order to be consistent with the integer values of open channel number, Mino and colleagues [29] implemented Fox and Lu's gate-based LA [16] with the calculated values of channel number rounded down to the nearest integer. Whereas Bruce [19] suggested that it would be more accurate to round to the nearest integer for the same LA. In the current work, we discuss the discretization of the channel open fractions for a channel-based LA [28]. A special rounding is chosen and applied to the open fractions. We show that, with the discretization treatment of the open fractions, the statistics of the membrane voltage and action potentials are improved for the channel number in the interval of [10, 100].

2. Methods

The neuron membrane voltage for the deterministic HH model is given by the following equation [14]:

$$-C\frac{dV}{dt} = I_{\mathrm{Na}} + I_{\mathrm{K}} + I_L - I_{Stim} \tag{1}$$

where V is the membrane potential, C the membrane capacitance, and I_{Stim} the stimulus current. $I_{\mathrm{Na}} = g_{\mathrm{Na}}hm^3(V - E_{\mathrm{Na}})$, $I_{\mathrm{K}} = g_{\mathrm{K}}n^4(V - E_{\mathrm{K}})$, and $I_L = g_L(V - E_L)$ are currents of Na^+ channels, K^+ channels, and leakage, respectively. The equations for the gating variables (i.e. n for K^+ channel, m and h for Na^+ channel), as well as the model parameters, can be found in Ref. [30].

Because of the thermal noise the channel subunits open and close stochastically. One can simulate the stochastic dynamics of each single gate (n, m and h gates) by an open/close two-state Markov process [31]. In detail, all the gates of the channels in the system are traced and updated for every small time step Δt. If a gate is closed at time t, then the probability that it is open at time $t + \Delta t$ is $\alpha \cdot \Delta t$. If a gate is open at time t, then the probability that it is closed at time $t + \Delta t$ is $\beta \cdot \Delta t$. Random numbers homogeneously distributed in $[0, 1]$ are generated at each time step and compared with these transition probabilities to determine the gate state at each time step. Here, α and β are voltage-dependent transition rates of channel gates and their expressions can be found in Eqs. (6)–(11) of Ref. [28]. This gate-based Markov process is considered as a standard Markov method for stochastic channel dynamics in the Letter. The corresponding Langevin approaches are called gate-based LA [15–24].

Alternatively, each Na^+ and K^+ channel can also be modeled with a five-channel-state chain and an eight-channel-state chain as shown in Fig. 1, respectively. With the transition rates given in Fig. 1, a Markov process can be considered based on these channel states, which will give the same statistical results as the gate-based Markov method. The Langevin approaches for the channel-based Markov process are then called channel-based LA.

The channel-based LA of the HH model was introduced originally by Fox and Lu [15,16], in which the channel state fractions are governed by the following master equations

$$\frac{d\vec{X}}{dt} = A_{\mathrm{K}}\vec{X} + S_{\mathrm{K}}\vec{\xi}_{\mathrm{K}} \tag{2}$$

$$\frac{d\vec{Y}}{dt} = A_{\mathrm{Na}}\vec{Y} + S_{\mathrm{Na}}\vec{\xi}_{\mathrm{Na}} \tag{3}$$

where vector $\vec{X} = \{x_i\}$ ($\mathrm{i} = 0, 1, 2, 3, 4$ in Fig. 1(a)) and $\vec{Y} = \{y_{jk}\}$ ($j = 0, 1, 2, 3$ and $k = 0, 1$ in Fig. 1(b)) are the fraction vectors of

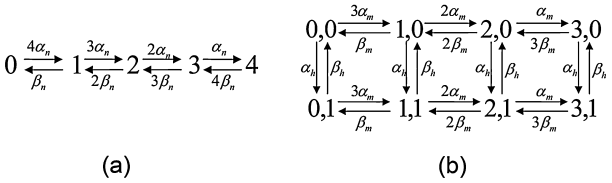

Fig. 1. The channel state diagram of (a) K^+ and (b) Na^+ channels. The numbers indicate how many subunits in a channel are in open state. For instance, in (a) the number 4 represents four open n subunits for an open K^+ channel and in (b) code 3,1 represents three open m subunits and one open h subunits for an open Na^+ channel. Arrows are labeled with voltage-dependent transition rates.

channel state. Matrices A_{K} and A_{Na} are the transition matrices; $\vec{\xi}_{\mathrm{K}}$ and $\vec{\xi}_{\mathrm{Na}}$ are noise vectors with each element an uncorrelated Gaussian white noise with zero mean and unit variance [32]; S_{K} and S_{Na} are the matrix square root of the diffusion matrix D_{K} and D_{Na}, respectively. The diffusion matrices D_{K} and D_{Na} and the transition matrices A_{K} and A_{Na} can be found in Ref. [23].

Because the noises in Eqs. (2) and (3) are Gaussian, the real-time values of x_i and y_{jk} may be negative. In order to have all elements positive in the matrices D_{K} and D_{Na}, the equilibrium fractions of x_i and y_{jk} are used in the diffusion matrix. Instead of directly calculating the square root of the diffusion matrix, the matrices S_{K} and S_{Na} can be simply expressed by the product of two matrices because the transitions among channel states are reversible [27], which can significantly reduce the computational time.

For numerical simulation, the difference Eq. of (2) is given by

$$\vec{X}^{t+\Delta t} = \vec{X}^t + \Delta t A_{\mathrm{K}}\vec{X}^t + \sqrt{\Delta t}S_{\mathrm{K}}\vec{\xi}_{\mathrm{K}}^t \tag{4}$$

There is a similar difference equation for the fraction vector $\vec{Y}$ in Eq. (3). In the following, this original channel-based LA will be referred as the unbounded LA (Unbound).

Since the fractions of channel states should not be out of range $[0, 1]$ we have suggested a bounded LA to confine the state fractions x_i and y_{jk} within $[0, 1]$ [28]. Take K^+ channel as an example, the numerical evolution of channel states can be expressed as follows.

$$\begin{aligned}\vec{X}^{t+\Delta t} &= \vec{X}^t + A_{\mathrm{K}}\vec{X}^t\Delta t + \left(S_{\mathrm{K}}\vec{\xi}_{\mathrm{K}}^t - \vec{\eta}_{\mathrm{K}}^t\right)\sqrt{\Delta t}\\ \vec{\eta}_{\mathrm{K}}^t &= \left(\vec{E}^{t+\Delta t} - \vec{E}^t\right)/\sqrt{\Delta t}\end{aligned} \tag{5}$$

where vector $\vec{\eta}_{\mathrm{K}}^t$ is the difference between two continuous truncated fractions ($\vec{E}^{t+\Delta t}$ and $\vec{E}^t$). The truncated fraction vector $\vec{E}$ is defined in Ref. [28]. This truncated and restored LA will be termed as the bounded LA (Bound) in the Letter.

The open fraction x_4 or y_{31} is continuous within $[0, 1]$ in the above two LAs. While the Markovian method gives a set of discrete values for open fraction. At large channel number the discrete values of state fractions can be nicely approximated by the continuous number, but at small channel number the continuous open fraction may introduce large errors for stochastic dynamics. Herein, we introduce furthermore a discretized scheme which is useful especially at small channel number.

For K^+ channel we consider the following method to discretize the channel open fraction:

$$x_4 = \begin{cases}(b_{\mathrm{K}} + 1)/N_{\mathrm{K}} & \text{if } a_{\mathrm{K}} > b_{\mathrm{K}} + \sigma_{\mathrm{K}}\\ b_{\mathrm{K}}/N_{\mathrm{K}} & \text{otherwise}\end{cases} \tag{6}$$

where $a_{\mathrm{K}} = x_4 N_{\mathrm{K}}$ and its integer part $b_{\mathrm{K}} = \mathrm{int}(x_4 N_{\mathrm{K}})$. Similarly, for Na^+ channel,

$$y_{31} = \begin{cases}(b_{\mathrm{Na}} + 1)/N_{\mathrm{Na}} & \text{if } a_{\mathrm{Na}} > b_{\mathrm{Na}} + \sigma_{\mathrm{Na}}\\ b_{\mathrm{Na}}/N_{\mathrm{Na}} & \text{otherwise}\end{cases} \tag{7}$$

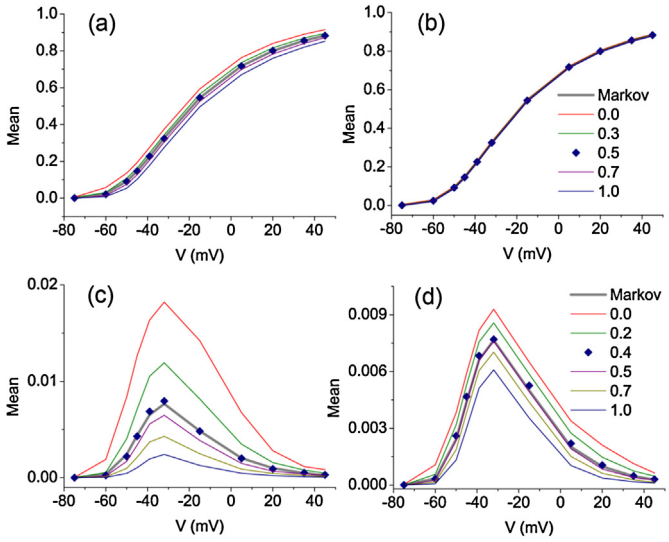

Fig. 2. Mean of voltage-clamp open fractions for K^+ and Na^+ channels with different values of σ_K (a)–(b) and σ_{Na} (c)–(d) as indicated. The left column is for $N = 10$ and the right column is for $N = 100$. Here $I_{Stim} = 0$ μA/cm^2.

where $a_{Na} = y_{31}N_{Na}$ and $b_{Na} = \text{int}(y_{31}N_{Na})$. Here σ_K and σ_{Na} are rounding parameters. After such a process, the discretized open fractions x_4 and y_{31} are applied in the calculation of channel currents. However, the continuous values of state fractions are still used in the equations for the calculations of diffusion matrices.

Setting the rounding parameters $\sigma_K = 0.5$ and $\sigma_{Na} = 0.5$ is a natural way, which corresponds to the rounding of open channel number to the nearest integer. But in this Letter, we set the rounding parameters $\sigma_K = 0.5$ and $\sigma_{Na} = 0.4$. The numerical simulation shows that with these rounding values the statistical properties of open fractions for dynamical action potentials can be best replicated. In Fig. 2, the means of open fractions for K^+ and Na^+ channels are calculated at clamped voltage V with $N = 10$ and 100 for different parameters σ_K and σ_{Na}. As shown in Figs. 2(a) and (b), the natural choice of $\sigma_K = 0.5$ provides best approximation to the mean open fractions of K^+ channels with Markov method; while the best approximation to the mean open fractions of Na^+ channels with Markov method is given at $\sigma_{Na} = 0.4$ for Na^+ channels, especially at small channel number $N = 10$ (Fig. 2(c)). Fig. 2 also indicates that the statistical open fraction of Na^+ channels is more sensitive to the rounding parameter than that of K^+ channels.

In the following, this discretization approach to the ion-channel open fractions will be called the discretized LA (Discrete). The mean is calculated over one simulation. The simulation time is 160 s, which is long enough compared with the typical duration (ms magnitude) of a generated action potential. The time step is 0.01 ms.

3. Results

In the model, we keep the density of Na^+ channels three times as big as that of K^+ channel [8]. By changing the membrane area, both the sodium and potassium channel numbers are changed. If not specified otherwise, the number N denotes the K^+ channel counts.

3.1. The stochastic trajectories of HH model

The stochastic channel open and closing dynamics will generate spontaneous action potentials even without any current stimulus. Fig. 3 plots the trajectories of the open fractions x_4 and y_{31} of Na^+ and K^+ channels, and the membrane voltage V for a channel system with $N = 10$ at $I_{Stim} = 0$ μA/cm^2. Here we compare

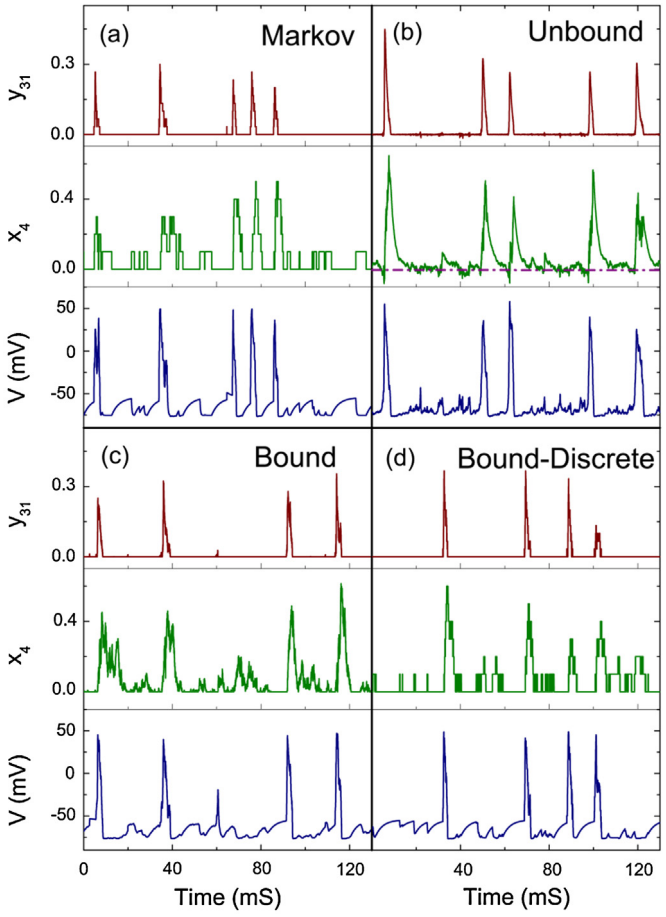

Fig. 3. Stochastic trajectories of the open fractions of K^+ and Na^+ channels and the voltage with (a) the Markovian method, (b) the unbounded LA, (c) the bounded LA and (d) the discretized LA. Here $N = 10$ and $I_{Stim} = 0$ μA/cm^2.

the stochastic behavior of the channel system obtained by different stochastic methods.

With the Markovian method, as plotted in Fig. 3(a), at both $x_4 = 0$ and $y_{31} = 0$ the membrane voltage increases slowly from its resting potential −75 mV because of the small depolarizing leakage current. A fluctuation of the open fraction x_4 at $x_4 = 0$ means a single K^+ channel to become open. The single-channel repolarizing K^+ current will rapidly drive the membrane potential back to its resting state. As a result, the subthreshold voltage shows a repetitive behavior of slow increase and rapid decrease.

With the unbounded LA in Fig. 3(b), before triggering an action potential, the open fraction x_4 of K^+ channel shows a much strong fluctuation around zero, sometimes positive and sometimes negative. A positive x_4 generates a small outward repolarizing K^+ current, while an unrealistic negative x_4 mathematically induces a small inward depolarizing K^+ current. As a result, with the unbounded LA the action potentials can be induced by large negative fluctuation of x_4, giving an unrealistic trigger dynamics.

With the bounded LA (Fig. 3(c)), the negative value of x_4 is forbidden, and so there is no more the unrealistic inward depolarizing K^+ current. But the open fraction x_4 of K^+ channel still shows frequently small fluctuations above zero at subthreshold state.

However, with the discretized LA, as shown in Fig. 3(d) the fluctuations of both x_4 and y_{31} are no more continuous, but are changed in steps. With this approach, upon a little depolarized potential above −75 mV, only a certain large fluctuation of y_{31} at $y_{31} = 0$ can cause a single Na^+ channel open to trigger an action potential. The discretization procedure in this approach can better mimic the trigger behavior of the Markovian channel dynamics.

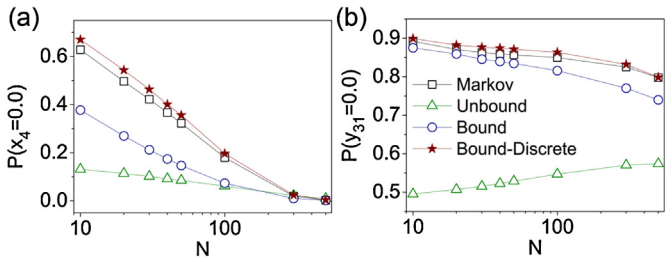

Fig. 4. Closing probabilities of ion channels. The probabilities (a) $P(x_4 = 0)$ and (b) $P(y_{31} = 0)$ that all K^+ and Na^+ channels are closed are plotted against N at $I_{Stim} = 0.0$ μA/cm^2. In all the figures, the squares, triangles, circles and stars represent the simulation results obtained by Markov method, unbounded LA, bounded LA and discretized LA, respectively.

3.2. Closing probabilities of ion channels

To clearly show that the open fractions obtained by the discretized LA at resting potential −75 mV mimic the results given by Markovian method, we discuss the probabilities $P(x_4 = 0)$ and $P(y_{31} = 0)$ that all the K^+ channels and all the Na^+ channels are in closing state. Fig. 4 plots the probabilities $P(x_4 = 0)$ and $P(y_{31} = 0)$ against N from 10 to 500 at $I_{Stim} = 0.0$ μA/cm^2. One can see that two continuous approaches, especially the unbounded LA, show incorrect $P(x_4 = 0)$ and $P(y_{31} = 0)$. On the other hand, the discretized LA gives good approximations to the results obtained by the Markov method.

3.3. Statistics of membrane voltage

Now we discuss the mean, ⟨V⟩, and standard deviation, DV, of voltage taken over the length of the simulation derived from different LAs. Two typical stimulus currents are studied, i.e., $I_{Stim} =$ 0.0 μA/cm^2 and $I_{Stim} = 15.0$ μA/cm^2, deterministically yielding a stable fixed point and a periodic oscillation, respectively. Note that, because the simulation program will breakdown at small N for unbounded LA with frequently unrealistic open fractions, the related simulation results only give for $N > 10$. As given in Fig. 5, the two continuous simulations, i.e. the unbounded LA and bounded LA, deviated from the standard values given by the Markov method at small channel number. In detail, the unbounded LA underestimates ⟨V⟩ at $N < 100$ and the bounded LA underestimates ⟨V⟩ at $N < 50$. On the other hand, the discretized LA captures the correct ⟨V⟩ even at $N = 5$. Discretized LA improves the estimation of DV compared with that of bounded LA at $I_{Stim} = 15.0$ μA/cm^2, but shows no evident improvement in the case of $I_{Stim} = 0.0$ μA/cm^2, indicating that discretization is more significant under high stimulus current.

A maximal and a minimal voltage are detected during each time window of 0.1 s, in which several action potentials will typically be observed. Then the averaged maximal and minimal voltages can be calculated for a long time recording. As a result, the averaged maximal and minimal voltages via constant stimulus current are plotted in Fig. 6. As shown in Fig. 6(a) with $N = 10$, the unbounded LA gives a large averaged maximal voltage at weak stimulus, and the bounded LA produces a slightly small averaged maximal voltage at strong stimulus. Only the discretized LA shows a nice approximation. At $N = 100$ plotted in Fig. 6(b), all LA approaches provide accurate values.

3.4. Statistics of action potential

Next, we study the mean, ⟨T⟩, and standard deviation, DT, of spike–spike interval. Here, the definition of the action potential refers to the literature [28]. Fig. 7 indicates that, compared to the bounded LA, the discretized LA shows no obvious improvement at $I_{Stim} = 0.0$ μA/cm^2, but at $I_{Stim} = 15.0$ μA/cm^2 the discretized

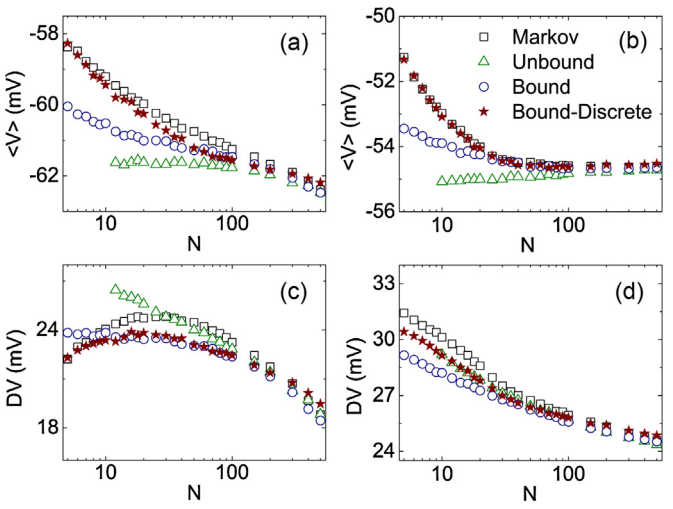

Fig. 5. The mean, ⟨V⟩, (a)–(b) and standard deviation, DV, (c)–(d) of the membrane voltage as a function of channel number N. Here, $I_{Stim} = 0.0$ and 15.0 μA/cm^2 are for the left and right columns, respectively.

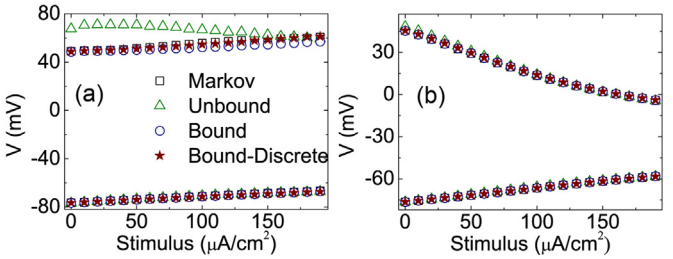

Fig. 6. Bifurcation diagram of the membrane voltage as a function of stimulus current. The averaged maximal (upper symbols) and minimal voltages (lower symbols) as a function of stimulus current for stochastic neuron model at (a) $N = 10$ and (b) $N = 100$.

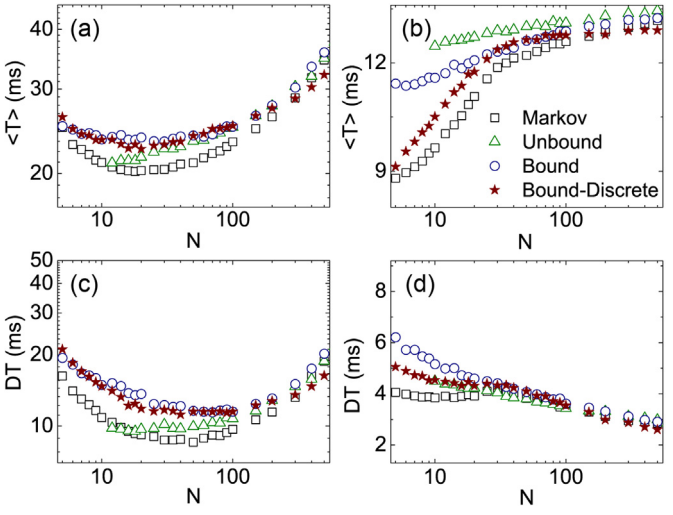

Fig. 7. The mean, ⟨T⟩ (a)–(b) and standard deviation, DT, (c)–(d) of the spike–spike interval as a function of channel number N. Here, $I_{Stim} = 0.0$ and 15.0 μA/cm^2 are for the left and right columns, respectively.

LA gives significantly enhanced results at small channel number (Fig. 7(b) and Fig. 7(d)), which again demonstrates the importance of discretization of open fractions for the cases with high stimulus current.

As to another two properties of action potential, namely spike amplitude and width, the discretized LA shows no improved statistics compared to the bounded LA (data not shown).

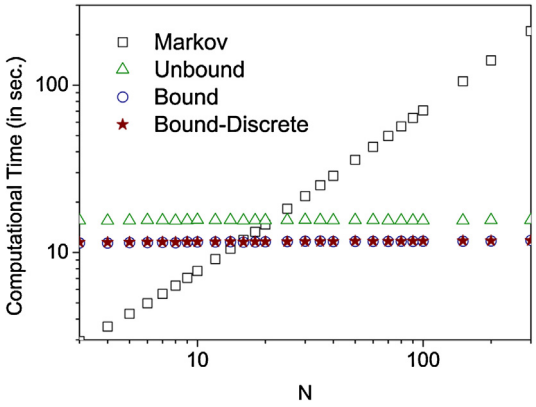

Fig. 8. The comparison of the computational performance. Here $I_{Stim} = 0.0\ \mu A/cm^2$. The time step is 0.01 ms and the simulation time is 40 sec.

3.5. Computational performance

Finally, we compare the computational performances of the Markov method and different LAs, as given in Fig. 8. The computational time is constant for each Langevin approach, while it linearly increases with N for the Markov method. The computational times of the bounded LA and the discretized LA are slightly reduced compared to the unbounded LA. This happens because the unbounded LA spends non-negligible additional time on the calculation of mean values of channel-state fractions. From Fig. 8, the cross point of Markov method and the discretized LA is about $N = 15$. As a consequence, when combined with the comparisons of LAs discussed above, this result indicates that for small membrane patch area, especially in $15 < N < 50$, the discretized LA would be an appropriate method to discuss the stochastic channel dynamics.

4. Discussions

In this Letter, we incorporate the discretization of open fractions of ion channels into a channel-based Langevin approach that we suggested previously in Ref. [28] in order to discuss the stochastic channel dynamics with small channel number. Mino's rounding down to the integer part [29] and Bruce's rounding to the nearest integer [19] are two special cases of the current approach. From the estimations of the mean and standard deviation of membrane voltage and spike–spike interval, we here show that the discretization method extends the valid region of channel number to a much smaller level around 10 K^+ channels. Furthermore, the computational cost of the channel-based Langevin approach is low, which makes it applicable for the channel system even with small channel number.

With the discussion of the detailed channel trajectories and of the probability for all channels to be in the closed state, we pinpoint a better estimation by the discretized approach to originate from the better simulation of trigger events of action potentials. For the system with small channel number, the first open Na^+ channel plays an important role to trigger an action potential. The discretization procedure in our Langevin approach can better mimic the trigger behavior of the stochastic channel dynamics, giving an improved stochastic description at small channel number. From the calculations of the mean and standard deviation of open fractions of Na^+ channels, we found that the open fraction of Na^+ channels is sensitive to parameter sigma, thus it's of importance for Na^+ channel to choose a proper sigma with respect to the adopted continuous LA.

Previous research has revealed the occurrence of stochastic resonance and the coherence of spikes caused by ion-channel noise for very small patch size [33]. The stochastic channel dynamics are found not only in neuronal dynamics, but also in the intracellular calcium signaling system [11,34,35]. It was found that the inositol 1,4,5-trisphosphate receptor channels are distributed in clusters with about several or several tens of channels on endoplasmic reticulum. We suggest that this discretization process can be applied to other theories with Langevin approaches and for other stochastic channel systems.

Acknowledgements

Yandong Huang and J.W. Shuai acknowledge support from the China National Funds for Distinguished Young Scientists under grants 11125419 and 10925525 and the Funds for the Leading Talents of Fujian Province. S. Rüdiger acknowledges financial support from the Deutsche Forschungsgemeinschaft (IRTG 1740 and RU1660). Computational supports from the Key Laboratory for Chemical Biology of Fujian Province, Xiamen University and Xiamen Super Computing Center are gratefully acknowledged.

References

[1] M.C.W. van Rossum, B.J. O'Brien, R.G. Smith, J. Neurophysiol. 89 (2003) 2406.
[2] G. de Vries, A. Sherman, J. Theor. Biol. 207 (2000) 513.
[3] K. Diba, H.A. Ester, C. Koch, J. Neurosci. 24 (2004) 9723.
[4] R.C. Cannon, C. O'Donnell, M.F. Nolan, PLoS Comput. Biol. 6 (2010) e1000886.
[5] T. Krogh-Madsen, L. Glass, E.J. Doedel, M.R. Guevara, J. Theor. Biol. 230 (2004) 499.
[6] C. Lerma, T. Krogh-Madsen, M. Guevara, L. Glass, J. Stat. Phys. 128 (2007) 347.
[7] A.A. Faisal, S.B. Laughlin, PLoS Comput. Biol. 3 (2007), e79.
[8] P. Jung, J.W. Shuai, Europhys. Lett. 56 (2001) 29.
[9] J.W. Shuai, P. Jung, Phys. Rev. Lett. 95 (2005) 114501.
[10] J.W. Shuai, P. Jung, Phys. Rev. Lett. 88 (2002) 68102.
[11] J.W. Shuai, P. Jung, Proc. Natl. Acad. Sci. USA 100 (2003) 506.
[12] J.W. Shuai, R. Sheng, P. Jung, Phys. Rev. E 81 (2010) 051913.
[13] S. Rüdiger, J.W. Shuai, I.M. Sokolov, Phys. Rev. Lett. 105 (2010) 048103.
[14] A.L. Hodgkin, A.F. Huxley, J. Physiol. 117 (1952) 500.
[15] R.F. Fox, Y.N. Lu, Phys. Rev. E 49 (1994) 3421.
[16] R.F. Fox, Biophys. J. 72 (1997) 2068.
[17] G. Schmid, I. Goychuk, P. Hanggi, Europhys. Lett. 56 (2001) 22.
[18] Y.D. Huang, S. Rüdiger, J.W. Shuai, Eur. Phys. J. B 83 (2011) 401.
[19] I. Bruce, Ann. Biomed. Eng. 35 (2006) 315.
[20] I. Bruce, Ann. Biomed. Eng. 37 (2009) 824.
[21] S. Zeng, P. Jung, Phys. Rev. E 70 (2004) 011903.
[22] B. Sengupta, S.B. Laughlin, J.E. Niven, Phys. Rev. E 81 (2010) 011918.
[23] J.H. Goldwyn, N.S. Imennov, M. Famulare, E. Shea-Brown, Phys. Rev. E 83 (2011) 04190801.
[24] M. Guler, Neural Comput. 25 (2013) 46.
[25] D. Linaro, M. Storace, M. Giugliano, PLoS Comput. Biol. 7 (2011) e1001102.
[26] J.H. Goldwyn, E. Shea-Brown, PLoS Comput. Biol. 7 (2011) e1002247.
[27] C.E. Dangerfield, D. Kay, K. Burrage, Phys. Rev. E 85 (2012) 051907.
[28] Y.D. Huang, S. Rüdiger, J.W. Shuai, Phys. Rev. E 87 (2013) 012716.
[29] H. Mino, J.T. Rubinstein, J.A. White, Ann. Biomed. Eng. 30 (2002) 578.
[30] P. Dayan, L. Abbott, Theoretical Neuroscience: Computational and Mathematical Modeling of Neural Systems, The MIT Press, Cambridge, 2001.
[31] D.T. Gillespie, J. Phys. Chem. 81 (1977) 2340.
[32] A. Papoulis, S.U. Pillail, Probability, Random Variables, and Stochastic Processes, fourth ed., McGraw-Hill Science/Engineering/Math., Columbus, 2002.
[33] M. Ozer, Phys. Lett. A 354 (2006) 258.
[34] I.F. Smith, S.M. Wiltgen, J.W. Shuai, I. Parker, Sci. Signal. 2 (2009) ra77.
[35] J.W. Shuai, Y.D. Huang, S. Ruediger, Phys. Rev. E 81 (2010) 041904.